PUBLISHED VERSION

Sun, Zhiwei; Nathan, Graham; Alwahabi, Zeyad T.; Dally, Bassam Single-shot, time-resolved planar laser-induced incandescence (TR-LII) for soot particle sizing - part II: in a turbulent flame Proceedings of the Australian Combustion Symposium, Perth, WA, 6-8 November 2013 / Mingming Zhu, Yu Ma, Yun Yu, Hari Vuthaluru, Zhezi Zhang and Dongke Zhang (eds.): pp.100-103

The copyright of the individual papers contained in this volume is retained and owned by the authors of the papers.

PERMISSIONS

http://www.anz-combustioninstitute.org/local/papers/ACS2013-Conference-Proceedings.pdf

Reproduction of the papers within this volume, such as by photocopying or storing in electronic form, is permitted, provided that each paper is properly referenced.

The copyright of the individual papers contained in this volume is retained and owned by the authors of the papers. Neither The Combustion Institute Australia & New Zealand Section nor the Editors possess the copyright of the individual papers.

Clarification of the above was received 12 May 2014 via email, from the Combustion Institute anz

12 May 2014

http://hdl.handle.net/2440/82571

Single-shot, time-resolved planar laser-induced incandescence (TR-LII) for soot particle sizing – Part II: in a turbulent flame

Z.W. Sun[1, 2, *], G.J. Nathan[1, 2], Z.T. Alwahabi[2, 3] and B. Dally[1, 2]
[1]School of Mechanical Engineering, University of Adelaide
[2]Center of Energy Technology, University of Adelaide
[3]School of Chemical Engineering, University of Adelaide

Abstract

Two dimensional measurements of the size of primary soot particles (d_p) is demonstrated in a turbulent flame, building on *Part I* of this paper *[Single-shot, time-resolved planar laser-induced incandescence (TR-LII) for soot particle sizing – Part I: in a laminar flame]*. The measurements were performed in a C_2H_4/air premixed, turbulent sooty flame, with the aim of demonstrating the potential of measuring the size of primary soot particles in a turbulent flame with planar TR-LII. Instantaneous planar measurements of d_p have been performed at different height of the sooty flame and sample images are presented in the present work. Both statistical data and joint statistical measurements are calculated from these images at various locations, to reveal the relationship between d_p and soot volume fraction together with that between d_p and particle number density.

Keywords: soot, time-resolved, laser-induce incandescence, soot particle size, turbulent sooty flame

1. Introduction

Soot particles comprise aggregates of small, primary particles, the size of which depend on the chemical history of the soot. The measurement of this parameter is therefore important both to enable the advancement of understanding of the evolution of soot in a range of relevant environments and also the development and validation of predictive models. In turbulent flames, it is also highly desirable that such measurements be performed simultaneously in multiple dimensions. This is because turbulent flames are unsteady and because of the highly non-uniform distribution of soot within them, which is typically found in thin sheets. This contrasts laminar flames, whose steady nature means that single point measurements are sufficient. In addition, the highly unsteady and non-uniform properties of turbulent flames hinders the application of sampling techniques such as scattering electron microscopy (SEM) and transmission election microscopy (TEM) that are used in laminar flames to characterize soot size and morphology [1] (and references therein). The first approach capable of planar measurement of the primary size of soot particles (d_p) has been presented in Part I of this paper using time-resolved planar laser-induced incandescence (TR-LII) [2]. However, that investigation only assessed the method in a laminar (premixed flame) environment. Hence there is a need to assess the suitability of the method in a turbulent flame. The present investigation aims to meet this need.

In spite of the growing number of measurements of soot volume fraction have been performed in turbulent flames [3-7], few measurements have been reported of soot particle size in turbulent flames. Of these, the RAYLIX method developed by Bockhorn and co-workers [6] is perhaps the best known. However, this technique does not the measure the primary size of soot particles and, in addition, its measurement uncertainty is unknown. Of particular interest are measurements of joint statistics, such as of d_p and soot volume fraction (*SVF*) or of d_p and soot number density (*N*). To the best of our knowledge, no well resolved measurements of these parameters have been reported previously in turbulent flames. Hence the aim of the present work is to provide new insight into the distribution of d_p within a turbulent flame by measurements of these statistics.

2. Experimental arrangement

The detailed descriptions of the process of deriving d_p from four successive images separated by time-steps of order 10 nanoseconds can be found in *Part I* [2]. The optical arrangement was also the same, with a laser

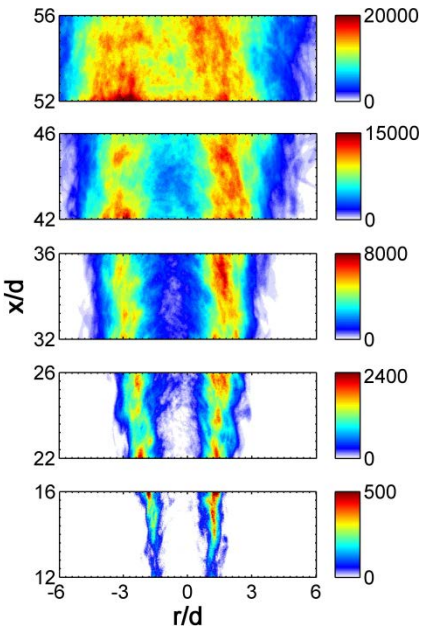

Figure 1. LII images averaged from 300 single-shot measurements at each height. Image intensities are shown by an arbitrary unit, which is the direct readout from the camera.

* Corresponding author:
Phone: (+61) 8 83132310
Email: zhiwei.sun@adelaide.edu.au

power of 0.13 J/cm^2 used in all measurements. The value of d_p was calculated from a model of the TR-LII signal at each pixel, which requires the temperature of the surrounding gas phase there. While future work will use a simultaneous measurement by two-line atomic fluorescence TLAF [8] to determine these values, for the present case the gas-phase temperature is assumed to be constant everywhere at 1700 K. Under this assumption, an uncertainty of ± 200 K of the assumed flame temperature (i.e., 1700 K) can result in an uncertainty of ± 3 nm for d_p = 15 nm or ± 5 nm for d_p = 40 nm, which are theoretically estimated using the LII model. The present measurement is also obtained from the ratio of two steps in the time-resolved LII signal decay. To reduce the uncertainty of this measurement, three simultaneous measurements of this value are obtained at each point using four images, each recording different stages of the time-resolved LII signal decay. The true value is taken the mean of these three simultaneous measurements, while the uncertainty is determined from their RMS.

Measurements were performed in a diffusion atmospheric-pressure C_2H_4/air jet flame issuing from a pipe (inner diameter d = 5.0 mm, outer diameter D = 6.7 mm). The flow rate of C_2H_4 was kept at 9.0 standard litres (Ls)/min while that of air was kept at 8.0 Ls/min for the air stream, resulting in a fuel equivalence ratio (φ) of 12.7 and a jet exit Reynolds number of 4500. The pipe was traversed vertically through the optics to allow measurement at five different heights from x/d = 12 to 56, where x is the flame height above the burner exit. The relative soot volume fractions at the five testing heights were characterized by the intensity of LII intensity averaged from 300 images, as shown in Fig. 1[1]. The lowest height at which soot particles are detected is in the range $12 < x/d < 16$, whereas strong signal is detected in the range $52 < x/d < 56$. In the upper region, strong LII signals are found in he central region of the jet flame, i.e., $r/d = 0$, where r is the radial distance from the jet central axis.

3. Results

3.1 Instantaneous size images

Figures 2 and 3 present a triplet of instantaneous images, comprising the LII measurement of relative soot volume fraction, the corresponding measurement of d_p and the root mean square (RMS) of the d_p measurement at the heights of $22 < x/d < 26$ and $52 < x/d < 56$, respectively. Spontaneous thermal emission from soot particles was also found in the raw images of LII signals (i.e., Figs. 2a and 3a). These spontaneous incandescent signals cause weak interferences to LII signals. Therefore, a threshold of 6% of the maximum value on each individual LII image was set to ensure that the size derivation process was only performed in the regions with high signal-to-noise ratios (S/N) of LII signals. Several important observations can be made. First is the clear trend that d_p increases with the flame height (x/d) (Figs. 2b and 3b). This reveals the growth process of primary soot particles, which is expected. Also, the RMSs of the instantaneous measurements, as shown in Figs. 2c and 3c, are mostly low, providing confidence in the measurement. The few locations of relatively high RMS is found at the edge of soot sheets, which is mostly due to the low intensities of LII signal there.

Next we turn to the relative distributions of d_p (central image) and soot volume fraction, *SVF*, (upper image). It is readily apparent that there is poor correlation between these two parameters. While *SFV* tends to peak near to the middle of a given soot sheet, there are several locations at which d_p tends to grow with distance through the sheet, while in others d_p tends to be larger in thicker

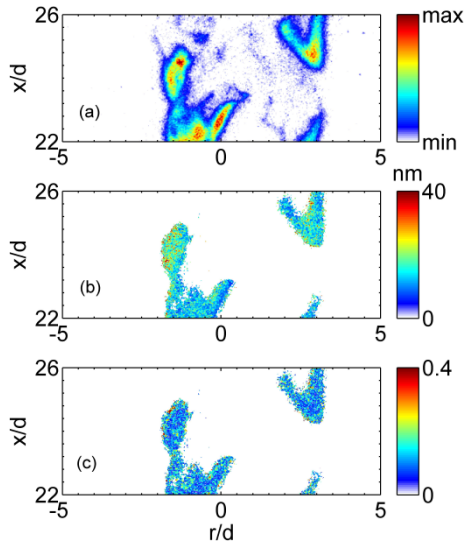

Figure 2. Instantaneous images of (a) LII raw signals, (b) the size of primary particles and (c) the corresponding root mean square (RMS) of the primary particle size measurement at $22 < x/d < 26$.

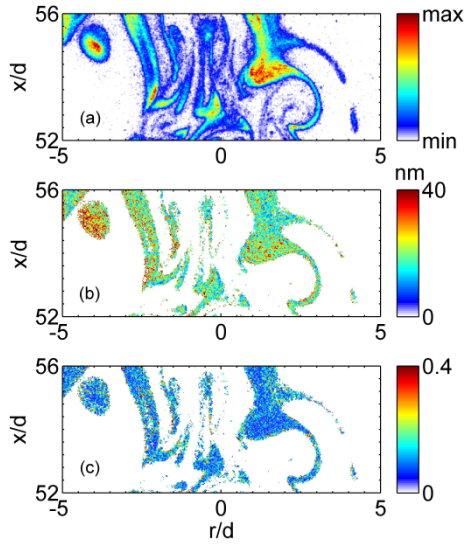

Figure 3. Instantaneous images of (a) LII raw signals, (b) the size of primary soot particles and (c) the corresponding root mean square (RMS) of the primary particle size measurement at $52 < x/d < 56$.

[1] It is well acknowledged that the intensity of LII signals is proportional to the soot volume fraction, which is described as $S(LII) = c \cdot SVF$, where c is a scaling factor. However, in experiments here, the factor c was not determined through a calibration process. Therefore, the LII images only, but still can, represent the relative *SVF* in the present work.

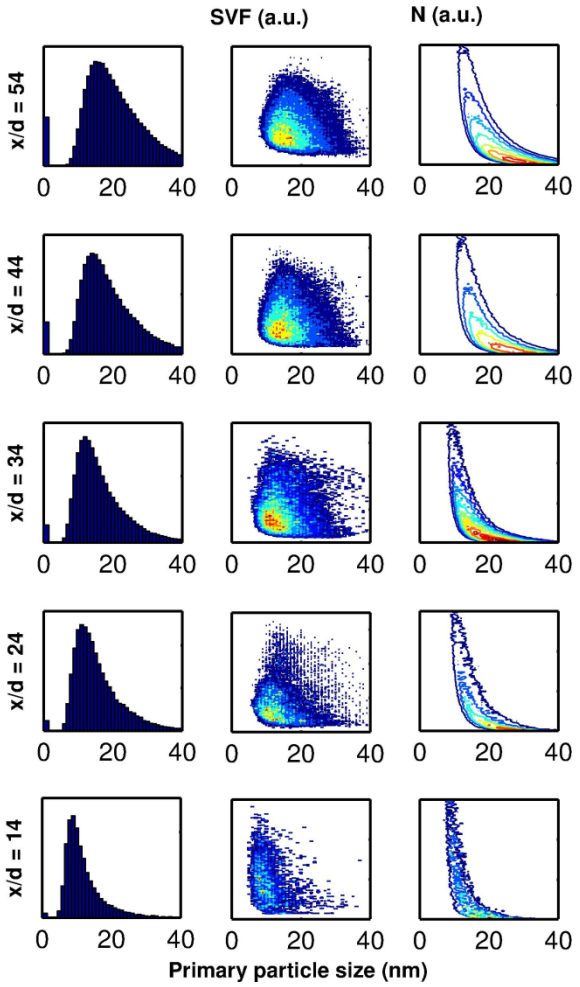

Figure 4. (from left to right) the probability distribution of the soot particle size, (d_p), joint statistics of soot volume fraction (*SVF*) and soot number density (*N*) conditioned on local size of primary soot particle at the five heights (*x/d*) investigated.

sheets. These observations, although preliminary, highlight the importance of 2D measurements, since such information could not be obtained from single-point measurements.

3.2 Statistical results

Figure 4 presents triplets of statistical measurements obtained at five values of *x/d*. All statistics were obtained from all non-zero pixels in each of 10 instantaneous images at each height. The left image in each triplet is the probability distribution of d_p, the central image is joint probability of d_p and *SVF*, while the RH image is the joint probability of d_p and soot number density, *N*. It should be noted that *N* was derived by the formula of $SVF = N \cdot (d_p)^3$, by which relative *SVF*s can only result in the relative number density.

The probability distributions of d_p in Fig. 4 (left column) show that both the mean and peak values of d_p increase with the flame height, *x/d*. This is consistent with the growth of primary soot particles with flame propagation. The shape of joint probability of d_p and *SVF* (middle column) does not change dramatically with *x/d*, although the magnitude does, especially between *x/d* = 14 and 24 in the upstream region of the flame. Likewise, the joint probability of d_p and *N* exhibits similar shapes throughout the flame. It should be noted that the trends in absolute values of the probability peaks should be treated with caution in the present data due to the use of different ND filters in the LII measurements. Despite the value of the statistical measurements shown in Fig. 4, it is worth noting that the same data could also be obtained from single-point measurements. Importantly the relatively small differences in the shape of these statistics with position in the flame highlights the limited value of single point statistics in comparison with the greater information that could be obtained in the planar images shown in Figs. 2 and 3.

Figure 5 presents the equivalent statistical measurements as a function of *r/d*. These statistics were calculated from all non-zero pixels in 10 instantaneous images at the flame heights between *x/d* = 32 and 36. The distributions of d_p (left hand images) reveal an initial increase in d_p with *r/d*, followed by a rapid reduction in d_p with further increases in r/d, consistent with increased oxidation in the outer region of the flame. The maximum value of d_p is found at $r/d \sim 2$. This trend is consistent with that of the soot volume fraction, *SVF*, as shown in Fig. 1. At *r/d* = 4, near to the flame edge, only very small primary soot particles survive due to the oxidation of the fuel by the entrained ambient air. .

Because the results shown in Fig. 5 were measured with the same optical arrangement, the joint statistics at each *r/d* can be directly compared with each other (even though both *SVF* and *N* are relative measurements). Also worth noting is that both *SVF* and *N* are shown with the same colour scale for all locations. Since the soot number density and the number density are correlated with each other through the size of primary soot particles, which is expressed as $SVF = N \cdot (d_p)^3$, the following discussions are only focused on the joint statistic of d_p and *N*.

Near to the axis, *r/d* = 0, the size distribution is quite wide and the vast majority of primary particles have a diameter less than 20 nm. While the shape of the distribution does not change, the distribution shifts to significantly larger particles, with the majority of primary particles smaller than 40 nm at *r/d* = 2, while the number density of the small particles decreases. At *r/d* = 2, the joint statistics also show that the particles larger than 20 nm are dominant in these regions. However, the trend changes dramatically for *r/d* > 2. At *r/d* = 3, the large particles have become much less prevalent, while at *r/d* = 4, the size distribution is almost a delta function, comprising entirely small particles. Statistically, the maximum value of the number density, *N*, does not change greatly from *r/d* = 0 to 4, as shown in Fig. 5. This is consistent with the soot nucleation process [9] not being significant at any radial distance at this flame height.

4. Conclusions

The planar measurement of the size of primary soot particles, d_p, using TR-LII has been demonstrated to perform with similar efficacy in a turbulent flame as in a laminar flame. In particular, the RMS of the three independent measurements of soot diameter, performed simultaneously with the four cameras, was typically less

than 10%, giving confidence in the reliability of the measurement, while the magnitude of the measured values and the key trends were broadly as expected. At the same time, visual inspection of the instantaneous images suggests that d_p is weakly correlated with soot volume fraction, *SFV*, within a given soot sheet, but may correlate better with other parameters, such as soot sheet thickness or distance from the oxidizing part of the sheet. This highlights the potential advantages of planar measurement over single-point techniques in a turbulent flame.

The preliminary analysis from a limited sample also reveals some interesting trends. In particular, d_p is found both to increase with axial distance over the range $14 < x/d < 52$ and to first increase slightly with radial distance over the range $0 < r/d < 2$, but then to decrease dramatically toward the edge of the flame in the range $2 < r/d < 4$. The distribution of d_p is smaller at the base of the flame and increases with height. With variation in r/d it is found that the distribution of d_p first increases and then narrows greatly with the dramatic reduction in d_p toward the outer edge of the flame. The shape of the joint statistics, which were calculated over a relatively large spatial region here, also change more dramatically toward the outer edge of the flame than with axial extent. These trends are consistent with known trends in laminar flames, in which d_p increases with residence time in reducing environments and decreases through oxidizing environments, highlighting the importance of the measurement.

Future work will seek both to apply planar TR-LII to well characterized turbulent sooting flames [10] and to extend the diagnostic capability. In particular, the potential to combine elastic scattering techniques with TR-LII will be evaluated, with a view to providing information on aggregates of primary soot particles.

5. Acknowledgment

The Australian Research Council (ARC) is gratefully acknowledged for their funding support of this work and the current position of the first author.

6. References

[1]. K. Tian, F. Liu, M. Yang, K.A. Thomson, D.R. Snelling and G.J. Smallwood, P Combust Inst **31** (1) (2007) 861-868.

[2]. Z.W. Sun, Z.T. Alwahabi, G.J. Nathan and D. Bassam, Proceedings of the Australian Combustion Symposium **9** (2013)

[3]. M.E. Mueller, Q.N. Chan, N.H. Qamar, B.B. Dally, H. Pitsch, Z.T. Alwahabi, et al., Combust Flame **160** (7) (2013) 1298-1309.

[4]. N.H. Qamar, Z.T. Alwahabi, Q.N. Chan, G.J. Nathan, D. Roekaerts and K.D. King, Combust Flame **156** (7) (2009) 1339-1347.

[5]. M. Koehler, K.P. Geigle, W. Meier, B.M. Crosland, K.A. Thomson and G.J. Smallwood, Appl Phys B-Lasers O **104** (2) (2011) 409-425.

[6]. H. Geitlinger, T. Streibel, R. Suntz and H. Bockhorn, P Combust Inst **27** (1998) 1613-1621.

[7]. T. Ni, J.A. Pinson, S. Gupta and R.J. Santoro, Applied Optics **34** (30) (1995) 7083-7091.

[8]. Q.N. Chan, P.R. Medwell, P.A.M. Kalt, Z.T. Alwahabi, B.B. Dally and G.J. Nathan, P Combust Inst **33** (2011) 791-798.

[9]. H. Richter and J.B. Howard, Prog Energ Combust **26** (4-6) (2000) 565-608.

[10]. The international ISF workshop: http://www.adelaide.edu.au/cet/isfworkshop/.

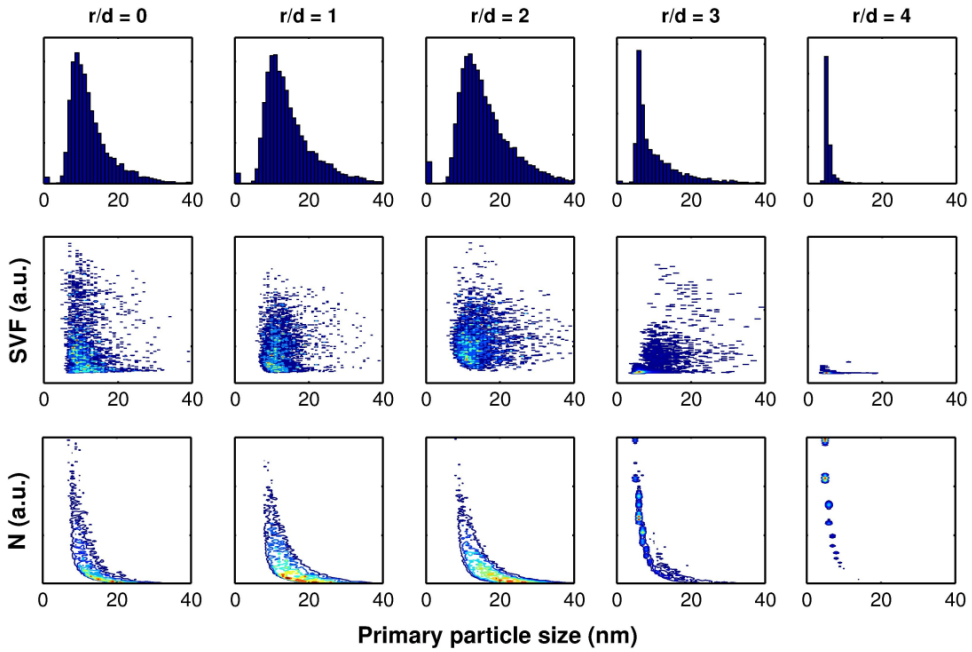

Figure 5. (from upper to lower) the probability distribution of the soot particle size, (d_p), joint statistics of soot volume fraction (*SVF*) and soot number density (*N*) conditioned on local soot particle size as a function of *r/d*. The statistics are performed at the height of *x/d* = 32 - 36. *SVF* and *N* are shown in the same scales in the joint statistics, respectively, and can be compared among the five radial distances.